

Controllability and maximum matchings of complex networks

Jin-Hua Zhao^{1*} and Hai-Jun Zhou^{1,2}

¹ CAS Key Laboratory of Theoretical Physics, Institute of Theoretical Physics,
Chinese Academy of Sciences, Beijing 100190, China and

² School of Physical Sciences, University of Chinese Academy of Sciences, Beijing 100049, China

(Dated: January 18, 2019)

Previously, the controllability problem of a linear time-invariant dynamical system was mapped to the maximum matching (MM) problem on the bipartite representation of the underlying directed graph, and the sizes of MMs on random bipartite graphs were calculated analytically with the cavity method at zero temperature limit. Here we present an alternative theory to estimate MM sizes based on the core percolation theory and the perfect matching of cores. Our theory is much more simplified and easily interpreted, and can estimate MM sizes on random graphs with or without symmetry between out- and in-degree distributions. Our result helps to illuminate the fundamental connection between the controllability problem and the underlying structure of complex systems.

I. INTRODUCTION

Graph theory and network science [1–6] provide a consistent framework to understand the structure and the dynamics of complex connected systems. In the past few years, the problems of controllability and control on complex networks and their application on real-world networked systems are among the main focuses of complex systems community [7–25]. A rather comprehensive review on control issues in complex systems can be found in [26]. Here we focus on a controllability problem that has been frequently studied in the recent network community, the controllability of linear-time invariant systems with nodal dynamics [7, 8]. In the paper [9], the problem of finding the minimal driver node sets (MDNSs) or the minimal actuator sets to steer system dynamics is mapped to the maximum matching (MM) problem [27] (finding a maximal set of edges with no shared vertices) on the bipartite representation of the underlying directed graph. On the analytical side, the cavity method at the zero temperature limit is derived to estimate MM sizes (size of a set of matched edges as a MM solution) [9, 15, 28–31]. On the simulation side, the Hopcroft-Karp algorithm [32] is adopted to find the MM solutions. Yet the analytical framework presented in [9] suffers from two points. First, the final equation connecting graph structure (the degree distribution) and MM sizes on random graphs [Eq. (S37)] is explicit, yet its derivation is quite complicated, burying a potentially simple and intrinsic explanation of the problem. Second, the degree asymmetry, or the disparity between out- and in-degree distributions, which is ubiquitous in real-world networked systems, is still not well fit in the above analytical framework, even its implication in controllability and MM sizes has been touched on in some of the literature [9, 12, 14].

In this paper, we try to resolve the above two points in a single framework. Our main contribution is the derivation of an alternative analytical framework to estimate

MM sizes on general random graphs based on the intuition of the Karp-Sipser algorithm [33, 34] and the related core percolation theory [35–38]. Our theory is much more simplified and easily interpreted. On random graphs with degree symmetry, our theory simply retrieves the result for MDNS sizes derived with the cavity method at the zero temperature limit in [9]. On random graphs without degree symmetry, our theory works naturally, thus provides an analytical perspective to the implication of degree asymmetry in the network controllability problem. In all, our framework helps to clarify a theoretical understanding of the roles of network topology and structure in the controllability of complex connected systems.

II. MODEL

We explain here the controllability and the MM problems on directed graphs. A directed graph $D = \{V, E\}$ consists of a vertex set V of a size $N (= |V|)$ and an arc set E of a size $M (= |E|)$ among vertices. An ordered pair $\{i, j\}$ of vertices i and j denotes an arc (a directed edge) starting from i and arriving at j . The undirected bipartite representation Γ of D is derived as follows: each vertex $i \in V$ is split into an out-vertex i^+ and an in-vertex i^- ; each arc $\{i, j\} \in E$ leads to an undirected edge (i^+, j^-) as an unordered pair of vertices; thus $\Gamma = \{V^+ \cup V^-, E^+\}$, in which V^+ , V^- , and E^+ are the out-vertex set, the in-vertex set, and the undirected edge set constructed as above, respectively. Once we find a MM of the undirected bipartite graph Γ , the unmatched vertices in the in-vertex set constitute a MDNS [9]. Specifically, $N_D = \max\{1, N - N_{MM}\}$ in which N_{MM} is the size of a MM and N_D is the size of the corresponding MDNS. On large graphs, we have $n_D = 1 - y$ in which $y (\equiv N_{MM}/N)$ is the relative size or the fraction of a MM and $n_D (\equiv N_D/N)$ is the relative size or the fraction of the corresponding MDNS. An illustration of the above notions is in Figs. 1 (a) to 1 (d).

On the simulation method to find MM solutions on undirected bipartite graphs, instead of the usually adopted Hopcroft-Karp algorithm [32], we adopt the

* Corresponding author: zhaojh190@gmail.com

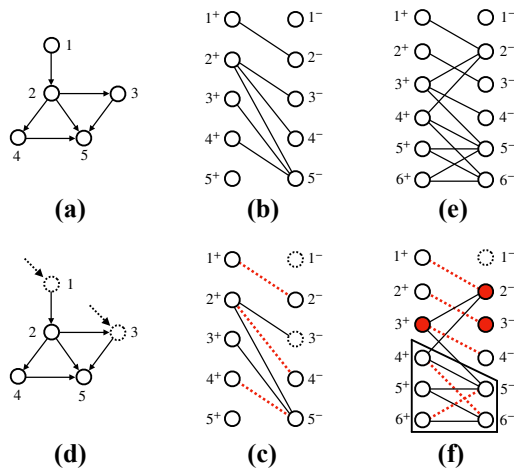


FIG. 1. An example of a directed graph, its bipartite representation, its MM and MDNS, and the Karp-Sipser algorithm on it. (a) A small directed graph with five vertices and six arcs. (b) The undirected bipartite representation of (a). (c) A MM of three edges in red dashed lines on the undirected graph in (b). Correspondingly, the in-vertices in dashed circles are unmatched. (d) A configuration of MDNS, in which the driver nodes or the actuators in dashed circles are simply the unmatched in-vertices in (c). (e) A bipartite representation of a hypothetical directed graph with six vertices and 12 arcs. (f) A MM of five edges in red dashed lines from the Karp-Sipser algorithm on the undirected graph in (e). The first stage of the GLR procedure consists of three elementary steps, after which the three red filled circles outside the trapezoid are roots and the five vertices and the 6 edges enclosed in this trapezoid form the core. The three dashed edges adjacent to these roots are matched edges constructed from the GLR procedure. In the core, a randomized edge removal procedure is applied as an edge $(4^+, 6^-)$ is removed and correspondingly matched. On the residual graph after the randomized edge removal procedure, the second stage of the GLR procedure involves only one elementary step, in which the root 5^- is removed. Correspondingly, an edge $(6^+, 5^-)$ [chosen randomly from $(5^+, 5^-)$ and $(6^+, 5^-)$] is matched. Till now the bipartite graph (f) leaves no edge and the set of dashed edges constitutes a matching for (e). The in-vertex 1^- in a dashed circle is the only unmatched vertex in the in-vertex set.

Karp-Sipser algorithm [33], which is basically a randomized local algorithm and finds MMs on a given undirected graph with high probability. A basic component of the Karp-Sipser algorithm is the greedy leaf removal (GLR) procedure, in which iteratively any vertex with only one nearest neighbor (a leaf) is removed along with its sole nearest neighbor (a root) in an elementary step. The GLR procedure leads to the core percolation on graphs [36, 37], and its original form and variants have implications in various combinatorial optimization and satisfiability problems [29, 30, 33, 34, 38–45]. The Karp-Sipser algorithm, an iterative process of the GLR procedures and the randomized edge removal procedures, is basically both a graph pruning process with vertex and edge

removals and a local algorithm to construct a matching. To construct a matching on a given graph, once an edge is matched and added into a matching, all the adjacent edges to its end-vertices are removed since, as the local constraint, there is at most one matched edge at which a vertex can be adjacent. On a general graph, the Karp-Sipser algorithm involves multiple stages of the GLR procedure, while in each stage the GLR procedure (with multiple elementary steps of removing a leaf and its neighboring root) is applied on the current graph to reveal its core. Correspondingly, in each elementary step of the GLR procedure, the edge between a root and its sole leaf or between a root and one of its multiple neighboring leaves is matched and added into a matching [33, 36]. On the core of the current graph, the randomized edge removal procedure is further applied, in which an edge in the core is randomly chosen and removed along with all the adjacent edges of the two end-vertices. Correspondingly, the removed edge is matched and added into a matching. The removal of an edge in a core possibly leads to newly generated leaves in the residual graph, thus triggers a new stage of the GLR procedure. Thus upon the iterative Karp-Sipser algorithm, a given graph shrinks to a graph without edges, correspondingly the matched edges constructed from the GLR procedures and the randomized edge removal procedures constitute an approximate MM of the given graph. An example of the Karp-Sipser algorithm is in Figs. 1 (e) and 1 (f).

III. THEORY

Here we derive an analytical framework to estimate the fraction of MMs on random undirected bipartite graphs. Before presenting our theory, we explain some graphical notions. On an undirected bipartite graph Γ of a directed graph D , for any edge (i^+, j^-) between an out-vertex i^+ and an in-vertex j^- , i^+ is a nearest neighbor of j^- , and vice versa. The degree of i^+ (j^-) in the out-(in-)vertex set k^{i^+} (k^{j^-}) is the size of its nearest neighbors in the in-(out-)vertex set $|\partial i^+|$ ($|\partial j^-|$). The degree distribution $P_+(k_+)$ [$P_-(k_-)$] of Γ is the probability of randomly finding a vertex with a degree k_+ (k_-) in the out-(in-)vertex set. The excess degree distribution $Q_+(k_+)$ [$Q_-(k_-)$] of Γ is the probability of arriving at a vertex with a degree k_+ (k_-) in the out-(in-)vertex set following a randomly chosen edge. The arc density c is defined as $c \equiv M/N$. We simply have the equivalence $Q_{\pm}(k_{\pm}) = k_{\pm}P_{\pm}(k_{\pm})/c$. When an edge (i^+, j^-) is removed from the original graph Γ , we consider the residual subgraph as the cavity graph $\Gamma \setminus (i^+, j^-)$. When an out-vertex i^+ (an in-vertex j^-) is removed along with all its adjacent edges from Γ , we consider the residual subgraph as the cavity graph $\Gamma \setminus i^+$ ($\Gamma \setminus j^-$).

Our analytical framework is based on the intuition of the Karp-Sipser algorithm and has two components: the core percolation theory and the perfect matching of cores. The core percolation theory [36–38] is the analytical the-

ory of the GLR procedure, which estimates the sizes of vertices in cores and roots as the two faces of the GLR procedure on both undirected and directed uncorrelated random graphs. We follow the language of the cavity method [28] to present the core percolation theory, in which the main results are basically marginal probabilities calculated from the stable solutions of pertinent cavity probabilities defined on random graphs. For the problem here on an uncorrelated random undirected bipartite graph Γ , a set of four cavity probabilities is introduced. Following a randomly chosen edge (i^+, j^-) arriving at the out-vertex i^+ , α^+ (β^+) is defined as the probability that i^+ becomes a leaf (a root) in the GLR procedure on the cavity graph $\Gamma \setminus (i^+, j^-)$; following a randomly chosen edge (i^+, j^-) arriving at the in-vertex j^- , α^- (β^-) is defined as the probability that j^- becomes a leaf (a root) in the GLR procedure on $\Gamma \setminus (i^+, j^-)$. On random undirected bipartite graphs without degree-degree correlations, with the locally tree-like structure approximation [28], we have the self-consistent equations for α^\pm and β^\pm .

$$\alpha^\pm = \sum_{k_\pm=1}^{\infty} Q_\pm(k_\pm)(\beta^\mp)^{k_\pm-1}, \quad (1)$$

$$\beta^\pm = 1 - \sum_{k_\pm=1}^{\infty} Q_\pm(k_\pm)(1 - \alpha^\mp)^{k_\pm-1}. \quad (2)$$

With the stable fixed solutions of (α^\pm, β^\mp) , we can calculate the fractions of out- and in-vertices in the core respectively as n^\pm , and the fraction of all roots in the out- and in-vertex sets as w .

$$n^\pm = \sum_{k_\pm=2}^{\infty} P_\pm(k_\pm) \times \sum_{s=2}^{k_\pm} \binom{k_\pm}{s} (\beta^\mp)^{k_\pm-s} (1 - \alpha^\mp - \beta^\mp)^s, \quad (3)$$

$$w = \left[1 - \sum_{k_+=0}^{\infty} P_+(k_+)(1 - \alpha^-)^{k_+} \right] + \left[1 - \sum_{k_-=0}^{\infty} P_-(k_-)(1 - \alpha^+)^{k_-} \right] - c\alpha^+\alpha^-. \quad (4)$$

The equation for n^\pm can be further simplified as follows. We first move the summation $\sum_{s=2}^{k_\pm}$ to $\sum_{s=0}^{k_\pm}$, then move the summation $\sum_{k_\pm=2}^{\infty}$ to $\sum_{k_\pm=0}^{\infty}$. With the equivalence $Q_\pm(k_\pm) = k_\pm P_\pm(k_\pm)/c$ and Eq. (1), we have a concise form for n^\pm .

$$n^\pm = \sum_{k_\pm=0}^{\infty} P_\pm(k_\pm) [(1 - \alpha^\mp)^{k_\pm} - (\beta^\mp)^{k_\pm}] - c\alpha^\pm(1 - \alpha^\mp - \beta^\mp). \quad (5)$$

Equations (1), (2), and (3) are first derived in [37], while Eq. (4) is our contribution here. We further present a simple explanation of the four equations. On a cavity graph $\Gamma \setminus i^+$ as $i^+ \in \Gamma$ is a randomly chosen out-vertex, the locally tree-like structure approximation assumes that the states (being leaves, roots, or trivial isolated vertices) of i^+ 's nearest neighbors or ∂i^+ are independent of each other in the GLR procedure. The same idea also applies on $\Gamma \setminus j^-$ upon a randomly chosen in-vertex j^- . We first consider the case from a cavity graph $\Gamma \setminus i^+$ to another cavity graph $\Gamma \setminus (i^+, j^-)$ after some edges are added in which (i^+, j^-) is a randomly chosen edge on Γ . If i^+ is a leaf on $\Gamma \setminus (i^+, j^-)$, its nearest neighbors other than j^- or simply $\partial i^+ \setminus j^-$ should be all roots on $\Gamma \setminus i^+$. The same logic also applies for j^- to be a leaf in $\Gamma \setminus (i^+, j^-)$. Thus we have Eq. (1). If i^+ is a root on $\Gamma \setminus (i^+, j^-)$, there should be at least one leaf in $\partial i^+ \setminus j^-$ on $\Gamma \setminus i^+$. The same logic also applies for j^- to be a root in $\Gamma \setminus (i^+, j^-)$. Thus we have Eq. (2). We then consider the case from a cavity graph $\Gamma \setminus i^+$ to the original graph Γ after some edges are added in which i^+ is a randomly chosen out-vertex on Γ . If i^+ is in the core on Γ , then among all its nearest neighbors or simply ∂i^+ on $\Gamma \setminus i^+$, there should be no leaves and also at least two vertices in the core to forbid the GLR procedure. The same logic also applies for j^- to be in the core on Γ . Thus we have Eq. (3). If i^+ is a root on Γ , there should be at least one leaf in ∂i^+ on $\Gamma \setminus i^+$. The same logic also applies for j^- to be a root on Γ . Yet a recounting happens in which the contribution of an isolated edge to a matching is counted twice. For example, see the isolated edge $(2^+, 3^-)$ in Figs. 1 (e) and 1 (f). To calculate the probability of the formation of isolated edges, we consider the case from a cavity graph $\Gamma \setminus (i^+, j^-)$ to the original graph Γ after the edge (i^+, j^-) is added in which (i^+, j^-) is a randomly chosen edge on Γ . If (i^+, j^-) is an isolated edge on Γ , both i^+ and j^- should be leaves on $\Gamma \setminus (i^+, j^-)$. Thus we have Eq. (4).

Here we explain a little more on the configurations of core and roots on an undirected bipartite graph. The core from the GLR procedure is well defined [36], that is to say, the configuration of a core is independent of the pruning process. Thus it is reasonable to quantify the fractions of out- and in-vertices in a core respectively as n^\pm . Yet the configuration of the roots is dependent on the pruning process. For example, a specific pruning process, in which all leaves in the in-vertex set trigger GLR steps before the leaves in the out-vertex set, simply leads to a larger size of out-vertices as roots on an undirected bipartite graph with degree symmetry. Yet the size of all roots of a bipartite graph, on average, is independent of the pruning process of the GLR procedure [36]. This is why we calculate the fraction of roots on a whole graph as w rather than distinguishing fractions of roots in the out- and in-vertex sets as w^\pm .

The second component of our analytical framework is the perfect matching of the core structure [27, 33]. On an undirected bipartite graph Γ , in the case of $n^+ > n^-$,

the perfect matching states that the in-vertices in the core are all matched, leading to the MM fraction of the core structure simply as n^- . Vice versa for the case of $n^- > n^+$.

For a given random undirected bipartite graph Γ , summing the fraction of matched edges reconstructed from the roots of the GLR procedure, which is simply w , and the estimated fraction of matched edges in the core structure, which is just $\min\{n^+, n^-\}$, we have the fraction of MMs on Γ . Equivalently, we have

$$y = w + \min\{n^+, n^-\}. \quad (6)$$

Taken together, Eqs. (1), (2), (3), (4), and (6) constitute our analytical framework of MM fractions on random undirected bipartite graphs.

It is easy to see that, our theory assumes a general form of degree distributions $P_{\pm}(k_{\pm})$ for a random bipartite graph. In the case of degree symmetry, we have $P_+(k) = P_-(k)$ for any k . From Eqs. (1) and (2), we have $\alpha^+ = \alpha^-$ and $\beta^+ = \beta^-$, further leading to $n^+ = n^-$ from Eq. (3). Equation (6) can be equivalently formulated as

$$y = w + \frac{1}{2}(n^+ + n^-). \quad (7)$$

With Eqs. (3) and (4) inserted into the above equation, we have

$$\begin{aligned} 1 - y &= \frac{1}{2} \left\{ \left[\sum_{k_+=0}^{\infty} P_+(k_+) (1 - \alpha^-)^{k_+} + \sum_{k_+=0}^{\infty} P_+(k_+) (\beta^-)^{k_+} - 1 \right] \right. \\ &+ \left[\sum_{k_-=0}^{\infty} P_-(k_-) (1 - \alpha^+)^{k_-} + \sum_{k_-=0}^{\infty} P_-(k_-) (\beta^+)^{k_-} - 1 \right] \\ &\left. + c[\alpha^+(1 - \beta^-) + \alpha^-(1 - \beta^+)] \right\}. \quad (8) \end{aligned}$$

We can compare Eq. (8) with the result in [9]. We substitute the parameters w_1 in Eq. (S26) as α^+ , w_2 in Eq. (S27) as β^+ , \hat{w}_1 in Eq. (S29) as α^- , and \hat{w}_2 in Eq. (S30) as β^- . The MDNS fraction n_D of Eq. (S37) simply reduces to Eq. (8). Thus our theory retrieves the estimation of MDNS sizes on random directed graphs with degree symmetry based on the cavity method at zero temperature limit. At the zero temperature limit for a finite-temperature cavity method for a physical system, the inverse temperature $\beta \equiv 1/T$ with T as the temperature is assumed as $\beta \rightarrow \infty$. In this limit case, only the ground-state solutions (in our case, the MMs with the maximum fraction) contribute to the physical system. The cavity messages on random graph ensembles thus can be coarse-grained and alternatively denoted with the cavity probabilities describing the distribution of these coarse-grained values. Correspondingly, the self-consistent equations and the ground-state energy with

the cavity messages all reduce to those forms with the cavity probabilities, along with the topological property (degree distribution) of random graphs as input. An intuitive understanding of this correspondence of results here and in [9] is that our analytical approach as a combination of the core percolation theory and the perfect matching of cores is essentially a cavity calculation of MM sizes on random graphs directly at the zero temperature. An implication of this correspondence is that Eq. (S37) for n_D in [9] only applies on random directed graphs with degree symmetry, while our theory also applies on random directed graphs without degree symmetry. On graphs with degree asymmetry, adopting Eq. (7) rather than Eq. (6) leads to an overestimation of y by $|n^+ - n^-|/2$.

IV. RESULTS

We test the simulation (the GLR procedure and the Karp-Sipser algorithm) and our analytical framework on some model random directed graphs. The details of graph construction and simplified equations of our theory are left in Appendix A. First, we consider the random directed graphs with symmetric out- and in-degree distributions. Examples are the directed Erdős-Rényi random graphs [46, 47], the directed random regular graphs, and the directed scale-free networks [48] generated with the static model [49–51] with the same out-degree exponent γ^+ and in-degree exponent γ^- . See the results of y , n^{\pm} , and w in Figs. 2 (a) to 2 (c). We then consider two cases of random directed graphs with degree asymmetry. The first case involves a same form for the out- and in-degree distributions with different parameters: the directed scale-free networks generated with the static model with degree exponents $\gamma_+ \neq \gamma_-$. The second case involves different forms for the out- and in-degree distributions: the directed random graphs with a Poissonian out-degree distribution and a power-law in-degree distribution generated from the static model. See the result in Figs. 2 (d) to 2 (f). In Fig. 2, we can see that, generally speaking, results coincide well between finite-size simulation and infinite-size analytical theory, except in cases of power-law degree distributions with $\gamma_- < 3.0$ from the static model. This tendency of result discrepancy has a root in the intrinsic degree-degree correlations in the graph construction process. As from the analytical results in [51], graphs generated with the static model with a degree exponent γ are much like uncorrelated random graphs when $\gamma > 3.0$, while they show increasingly recognizable degree-degree correlation with decreasing γ when $\gamma < 3.0$.

From [37], on random directed graphs with degree symmetry, the degenerate solutions of $(\alpha^{\pm}, \beta^{\mp})$ experience a continuous decrease at the core percolation transitions, leading to a continuous emergence of core with nontrivial n^{\pm} , while on random directed graphs with degree asymmetry, the stable solution of (α^+, β^-) or (α^-, β^+) experi-

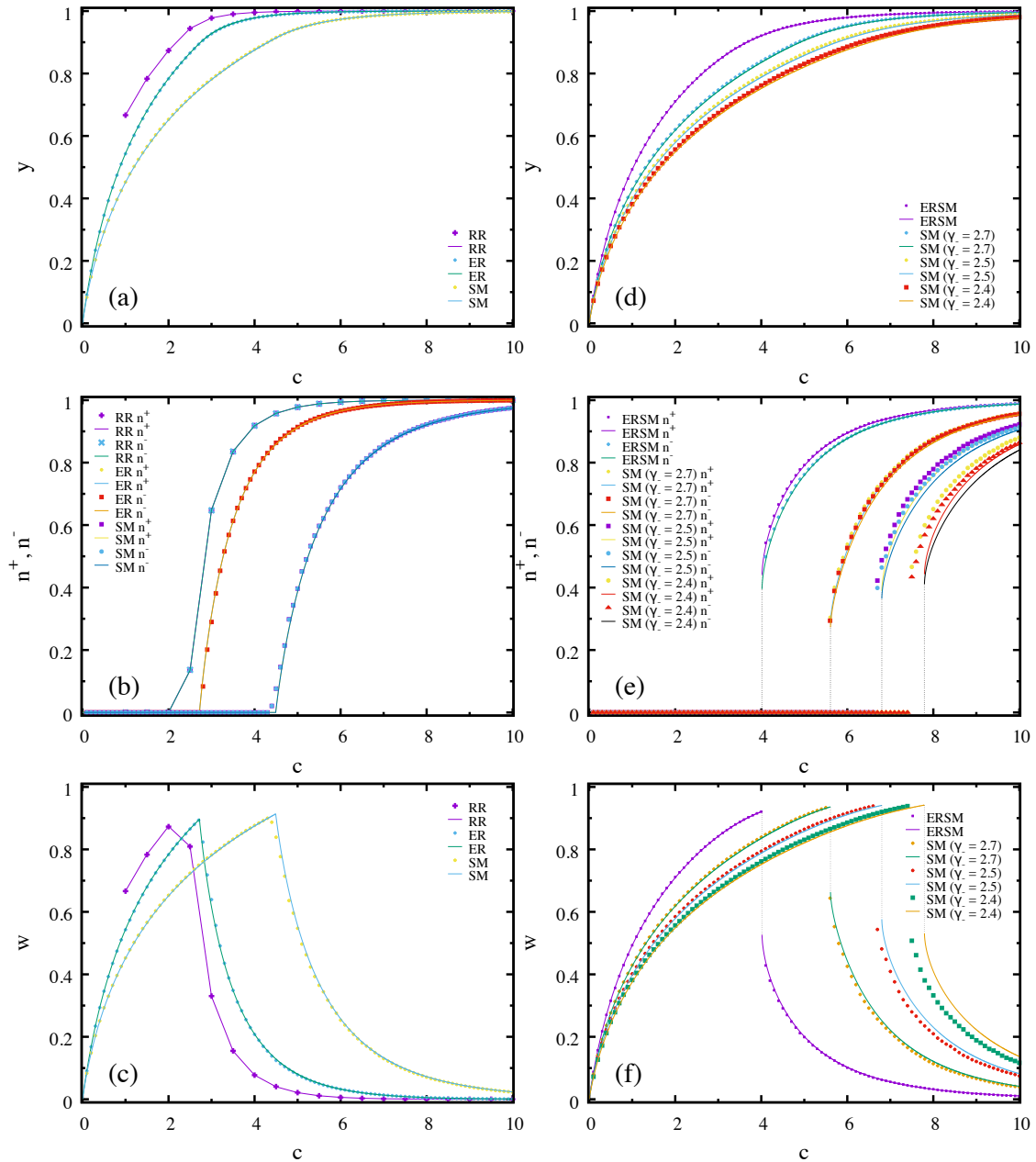


FIG. 2. The relative sizes of MM y , the fractions of out- and in-vertices in cores n^\pm , and the fraction of roots w on random directed graphs. (a) - (c) show results on the directed random regular (RR) graphs, directed Erdős-Rényi (ER) random graphs, and directed asymptotical scale-free networks generated with the static model (SM) with degree exponents $\gamma_+ = \gamma_- = 3.0$, which are listed from left to right, respectively. (d) - (f) show results on the random directed graphs with Poissonian out-degree distribution and power-law in-degree distribution with an exponent $\gamma_- = 3.0$ generated with the static model (ERSM) and the directed asymptotical scale-free networks generated with the static model (SM) with $\gamma_+ = 3.0$ and $\gamma_- = 2.7, 2.5, 2.4$, which are listed from left to right, respectively. (a) and (d) show results of y . (b) and (e) show results of n^\pm . (c) and (f) show results of w . Each sign is for the simulation result on a single graph instance with a vertex size $N = 10^5$. Each solid line is for the analytical result on infinitely large random graphs. Each dotted line in (e) and (f) is for a discontinuity in the analytical result.

ences a discontinuous drop at the core percolation transitions, leading to a discontinuous appearance of core with finite n^\pm by a gap. In Fig. 2, we can see that w follows a rise-and-fall pattern and undergoes a continuous decrease or a sudden drop with the same continuity of n^\pm at the

core percolation transitions. Here we give an intuitive understanding of the pattern of w and its behavior at the transition points. Before the formation of the giant connected component on a graph, there are mainly trees with leaves in the graph. The GLR procedure is carried

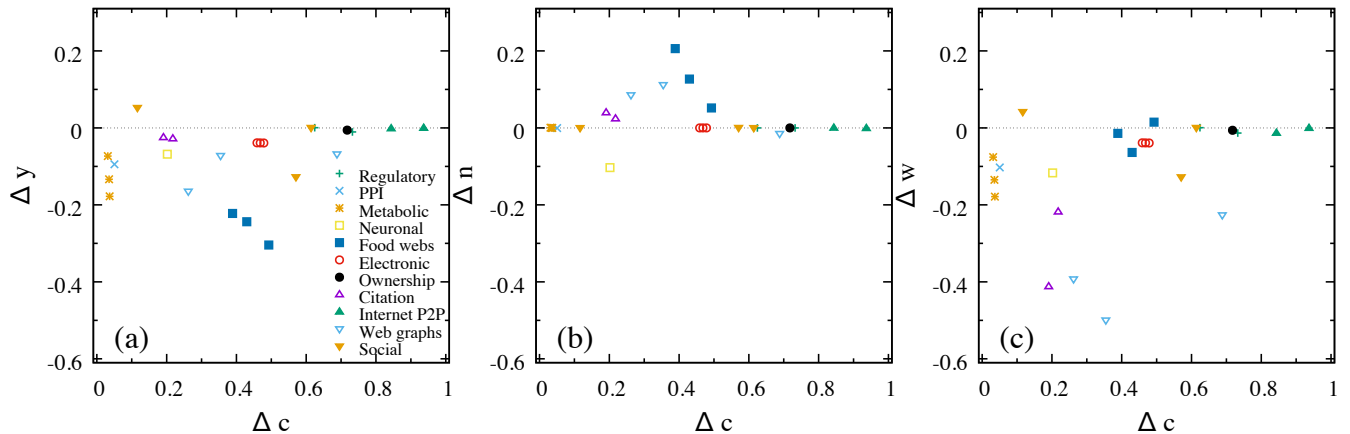


FIG. 3. The differences of the MM sizes Δy , the core asymmetries Δn , and the root sizes Δw between simulation and analytical theory on 24 real-world network instances. Δy , Δn , and Δw are shown against the degree asymmetry Δc in (a), (b), and (c), respectively.

out basically based on the existing leaves in the graph, during which more added edges lead to more leaves and more GLR steps, thus an increasing w . With more edges added into the graph after the formation of the giant connected component, newly revealed leaves in the iterative GLR procedure play an increasingly important role, in which a larger arc density c leads to more element-tray steps of the GLR procedure, thus an ever increasing w , until the formation of a core. A core is a subgraph which the GLR procedure cannot touch. A sudden emergence of core n^\pm at the core percolation transition simply leads to a macroscopic fraction of vertices $(n^+ + n^-)/2$ in the graph where the GLR procedure is excluded, thus a sudden drop of the root size w . With even more edges added into the graph beyond the core percolation transition, there is an increasing difficulty both in triggering the GLR procedure and generating new leaves. Thus an increasing n^\pm and a shrinking w happen at the same time with a growing arc density c .

We further apply the simulation and our theory on real-world networks. A description of a dataset of 24 network instances is in Appendix B. We focus on the effect of the degree asymmetry on the matching sizes. For a directed network instance D with degree distributions $P_\pm(k_\pm)$ for its undirected bipartite representation, we define a parameter to measure its degree asymmetry as $\Delta c \equiv \sum_{k=0}^{\infty} |P_+(k) - P_-(k)|/2$. It is easy to see that $\Delta c \in [0, 1]$, and a larger Δc corresponds to a larger disparity between the out- and in-degree distributions. We also define the core asymmetry towards out-vertices in cores as $\delta n \equiv n^+ - n^-$ as the difference between the sizes of the out- and in-vertex sets in a core after the GLR procedure. For any real-world network in the dataset, we count from simulation the fraction of MM y_{real} , the core asymmetry δn_{real} , and the fraction of roots w_{real} . We also calculate y_{theory} , δn_{theory} , and w_{theory} respectively with the analytical theory with the empirical out-

and in-degree distributions of the network instance as inputs. These analytical predictions based on empirical degree distributions can be approximately considered as averaged results of simulation on network instances with degree-constrained randomized wiring of arcs [9]. The difference $\Delta y \equiv y_{\text{real}} - y_{\text{theory}}$, $\Delta n \equiv \delta n_{\text{real}} - \delta n_{\text{theory}}$, and $\Delta w \equiv w_{\text{real}} - w_{\text{theory}}$ can be considered as measures of the deviation of real-world networks from their randomized versions from the perspectives of the GLR procedure and MM sizes. Results on the real-world network dataset are in Fig. 3. We can see that the 24 network instances show a wide range of degree asymmetry. For the core asymmetry difference Δn , 16 instances show trivial values, seven instances show clear positive values, and only one instance shows clear negative values. For the root size difference Δw , eight instances show trivial values, only one instance shows clear positive values, and the other 15 instances show clear negative values. For the MM size difference Δy , six instances show trivial values, only one instance shows clear positive values, and the other 17 instances show clear negative values. Taken the above results in short, we have two major observations. First, discernible nontrivial values of Δy , Δn , and Δw mainly appear in those instances with moderate and small degree asymmetries. Second, compared to their degree-constrained randomized counterparts, the network instances in our dataset show a rather clear tendency towards larger core asymmetries, smaller root sizes, and smaller MM sizes. We only present an empirical description of the results here. Further quantitative study on how the higher order structure in real networks affect on the deviation of core asymmetry and roots should be continued.

V. CONCLUSION

Establishing the relation between the network structural properties and the size of driver nodes or actuators to guide a dynamical system to any final state is a fundamental problem in the network controllability problem, which is a recent example of the intricate interplay between structure and function of complex networked systems. In this paper, we derive a simple alternative framework to estimate the fraction of MMs on directed systems, thus the size of MDNSs, a basic quantity of the network controllability problem. Our simulation method adopts the Karp-Sipser algorithm on the undirected bipartite representations of the underlying directed networks. Our analytical theory is based on the core percolation theory and the perfect matching of cores, which works on random graphs with or without degree symmetry. We also find that real-world network instances show a clear tendency to larger core asymmetry and smaller root sizes and MM sizes compared to their degree-constrained randomizations, which is worthy for further study. We hope that our theory contributes to clarify the fundamental role of the network structure in the controllability and control issues of complex connected systems.

VI. ACKNOWLEDGEMENTS

This research is supported by the National Natural Science Foundation of China (Grant No. 11747601) and the Chinese Academy of Sciences Grant QYZDJ-SSW-SYS018. J.-H.Z. is partially supported by the Key Research Program of Frontier Sciences Chinese Academy of Sciences (Grant No. QYZDB-SSW-SYS032) and the National Natural Science Foundation of China (Grant No. 11605288). J.-H.Z. thanks Professor Pan Zhang (ITP-CAS) for his hospitality.

VII. APPENDIX A: EQUATIONS ON MODEL RANDOM GRAPHS

A. Erdős-Rényi random graphs

For directed Erdős-Rényi (ER) random graphs [46, 47], a graph instance $D = \{V, E\}$ with a vertex set V of a size $N(= |V|)$ and an arc set E of a size $M(= |E|)$ can be constructed as the following: a null graph with N vertices and no edge is initialized; a number of M arcs are established by randomly choosing two distinct vertices, say vertices i and j , and connecting them with assigning a random direction with an equal probability, say $\{i, j\}$ or $\{j, i\}$.

On directed ER random graphs with arc density $c(\equiv M/N)$, we have the degree distributions and the excess degree distributions of their undirected bipartite representations as

$$P_{\pm}(k_{\pm}) = e^{-c} \frac{c^{k_{\pm}}}{k_{\pm}!}, \quad (9)$$

$$Q_{\pm}(k_{\pm}) = e^{-c} \frac{c^{k_{\pm}-1}}{(k_{\pm}-1)!}. \quad (10)$$

We have the summation rules with above equations as follows:

$$\sum_{k_{\pm}=0}^{\infty} P_{\pm}(k_{\pm}) x^{k_{\pm}} = e^{-c(1-x)}, \quad (11)$$

$$\sum_{k_{\pm}=1}^{\infty} Q_{\pm}(k_{\pm}) x^{k_{\pm}-1} = e^{-c(1-x)}. \quad (12)$$

Thus we have the simplified equations as follows.

$$\alpha^{\pm} = e^{-c(1-\beta^{\mp})}, \quad (13)$$

$$\beta^{\pm} = 1 - e^{-c\alpha^{\mp}}, \quad (14)$$

$$n^{\pm} = 1 - \alpha^{\pm} - \beta^{\pm} - c\alpha^{\pm}(1 - \alpha^{\mp} - \beta^{\mp}), \quad (15)$$

$$w = \beta^{+} + \beta^{-} - c\alpha^{+}\alpha^{-}. \quad (16)$$

B. Random regular graphs

A directed random regular (RR) graph instance $D = \{V, E\}$ with a vertex set V of a size $N(= |V|)$ and an arc set E of a size $M(= |E|)$ can be generated from its undirected counterpart: an undirected RR graph instance is constructed in which each vertex is connected to an integer $K(\equiv 2M/N)$ of randomly chosen distinct vertices; then each edge is assigned with a random direction with an equal probability.

For the directed RR graph instances with an arc density $c(\equiv K/2)$ as K is the integer degree of the underlying undirected RR graphs, we have the degree distributions as

$$P_{\pm}(k_{\pm}) = \binom{K}{k_{\pm}} / 2^K, \quad (17)$$

$$Q_{\pm}(k_{\pm}) = \binom{K-1}{k_{\pm}-1} / 2^{K-1}. \quad (18)$$

We have the summation as

$$\sum_{k_{\pm}=0}^K P_{\pm}(k_{\pm}) x^{k_{\pm}} = \left(\frac{1+x}{2}\right)^K, \quad (19)$$

$$\sum_{k_{\pm}=1}^K Q_{\pm}(k_{\pm}) x^{k_{\pm}-1} = \left(\frac{1+x}{2}\right)^{K-1}. \quad (20)$$

We thus have the simplified equations as

$$\alpha^\pm = \left(\frac{1 + \beta^\mp}{2}\right)^{K-1}, \quad (21)$$

$$\beta^\pm = 1 - \left(\frac{2 - \alpha^\mp}{2}\right)^{K-1}, \quad (22)$$

$$n^\pm = \left(\frac{2 - \alpha^\mp}{2}\right)^K - \left(\frac{1 + \beta^\mp}{2}\right)^K - \frac{1}{2}K\alpha^\pm(1 - \alpha^\mp - \beta^\mp), \quad (23)$$

$$w = 2 - \left(\frac{2 - \alpha^-}{2}\right)^K - \left(\frac{2 - \alpha^+}{2}\right)^K - \frac{1}{2}K\alpha^+\alpha^-. \quad (24)$$

C. Asymptotical scale-free networks

A random directed scale-free (SF) network $D = \{V, E\}$ with $N (= |V|)$ vertices and $M (= |E|)$ arcs follows degree distributions $P_+(k_+) \propto k_+^{-\gamma_+}$ and $P_-(k_-) \propto k_-^{-\gamma_-}$ in which γ_+ and γ_- are the out- and in-degree exponents, respectively. We adopt the static model [49–51] to generate asymptotical SF networks. We follow the procedure: a null graph with N vertices and no edge is initialized in which each vertex has an index $i (= 1, 2, \dots, N)$; each vertex is assigned with an out-weight $w_i^+ = \hat{w}_i^+ \equiv i^{-\xi_+}$ and an in-weight $w_i^- = \hat{w}_i^- \equiv i^{-\xi_-}$ as $\xi_\pm \equiv 1/(\gamma_\pm - 1)$; to further decouple the weights and the indices of vertices, the out-weights and in-weights are randomly shuffled between vertices respectively, then we have a new sequence of vertices with an out-weight w_i^+ and an in-weight w_i^- for each vertex i ; M arcs are added into the null graph, while in each step a vertex i is chosen randomly from the out-vertex set with a probability proportional to its out-weight w_i^+ , and a vertex j is chosen randomly from the in-vertex set with a probability proportional to its in-weight w_j^- , then an arc $\{i, j\}$ is established if there is no $\{i, j\}$ nor $\{j, i\}$ before.

A directed SF network instance generated with the static model with an arc density c , an out-degree exponent γ_+ , and an in-degree exponent γ_- has the degree distributions $P_\pm(k_\pm)$ as

$$\begin{aligned} P_\pm(k_\pm) &= \frac{1}{\xi_\pm} \frac{(c(1 - \xi_\pm))^{k_\pm}}{k_\pm!} \int_1^\infty dt e^{-c(1 - \xi_\pm)t} t^{k_\pm - 1 - 1/\xi_\pm} \\ &= \frac{1}{\xi_\pm} \frac{(c(1 - \xi_\pm))^{k_\pm}}{k_\pm!} E_{-k_\pm + 1 + 1/\xi_\pm}(c(1 - \xi_\pm)) \end{aligned} \quad (25)$$

The general exponential integral function $E_a(x) \equiv \int_1^\infty dt e^{-xt} t^{-a}$ can be calculated with the GNU Scientific Library (GSL) [52]. For large k_+ and k_- , we have $P_+(k_+) \propto k_+^{-\gamma_+}$ and $P_-(k_-) \propto k_-^{-\gamma_-}$, respectively. The excess degree distributions $Q_\pm(k_\pm)$ have the form

$$Q_\pm(k_\pm) = \frac{1 - \xi_\pm}{\xi_\pm} \frac{(c(1 - \xi_\pm))^{k_\pm - 1}}{(k_\pm - 1)!} E_{-k_\pm + 1 + 1/\xi_\pm}(c(1 - \xi_\pm)). \quad (26)$$

For the summation rules, we have

$$\sum_{k_\pm=0}^\infty P_\pm(k_\pm) x^{k_\pm} = \frac{1}{\xi_\pm} E_{1+1/\xi_\pm}(c(1 - \xi_\pm)(1 - x)), \quad (27)$$

$$\sum_{k_\pm=1}^\infty Q_\pm(k_\pm) x^{k_\pm - 1} = \frac{1 - \xi_\pm}{\xi_\pm} E_{\frac{1}{\xi_\pm}}(c(1 - \xi_\pm)(1 - x)) \quad (28)$$

We thus have the simplified equations as

$$\alpha^\pm = \frac{1 - \xi_\pm}{\xi_\pm} E_{\frac{1}{\xi_\pm}}(c(1 - \xi_\pm)(1 - \beta^\mp)), \quad (29)$$

$$\beta^\pm = 1 - \frac{1 - \xi_\pm}{\xi_\pm} E_{\frac{1}{\xi_\pm}}(c(1 - \xi_\pm)\alpha^\mp), \quad (30)$$

$$\begin{aligned} n^\pm &= \frac{1}{\xi_\pm} E_{1+1/\xi_\pm}(c(1 - \xi_\pm)\alpha^\mp) \\ &\quad - \frac{1}{\xi_\pm} E_{1+1/\xi_\pm}(c(1 - \xi_\pm)(1 - \beta^\mp)) \\ &\quad - c\alpha^\pm(1 - \alpha^\mp - \beta^\mp), \end{aligned} \quad (31)$$

$$\begin{aligned} w &= 2 - \frac{1}{\xi_+} E_{1+1/\xi_+}(c(1 - \xi_+)\alpha^-) \\ &\quad - \frac{1}{\xi_-} E_{1+1/\xi_-}(c(1 - \xi_-)\alpha^+) - c\alpha^+\alpha^-. \end{aligned} \quad (32)$$

D. Random graphs with different forms of out- and in-degree distributions

We can construct random directed graphs with a Poissonian out-degree distribution and a power-law in-degree distribution generated from the static model with an in-degree exponent γ_- . In the static model, we have $\xi_- \equiv 1/(\gamma_- - 1)$.

With equations in the previous subsections and the arc density c , we have the following simplified equations.

$$\alpha^+ = e^{-c(1 - \beta^-)}, \quad (33)$$

$$\alpha^- = \frac{1 - \xi_-}{\xi_-} E_{\frac{1}{\xi_-}}(c(1 - \xi_-)(1 - \beta^+)), \quad (34)$$

$$\beta^+ = 1 - e^{-c\alpha^-}, \quad (35)$$

$$\beta^- = 1 - \frac{1 - \xi_-}{\xi_-} E_{\frac{1}{\xi_-}}(c(1 - \xi_-)\alpha^+), \quad (36)$$

$$n^+ = 1 - \alpha^+ - \beta^+ - c\alpha^+(1 - \alpha^- - \beta^-), \quad (37)$$

$$\begin{aligned} n^- &= \frac{1}{\xi_-} E_{1+1/\xi_-}(c(1 - \xi_-)\alpha^+) \\ &\quad - \frac{1}{\xi_-} E_{1+1/\xi_-}(c(1 - \xi_-)(1 - \beta^+)) \\ &\quad - c\alpha^-(1 - \alpha^+ - \beta^+), \end{aligned} \quad (38)$$

$$w = \beta^+ + 1 - \frac{1}{\xi_-} E_{1+1/\xi_-}(c(1 - \xi_-)\alpha^+) - c\alpha^+\alpha^- \quad (39)$$

VIII. APPENDIX B: DESCRIPTION OF THE REAL NETWORK DATASET

We list some information about the real-world network dataset we use in the main text in table I. A major part of large network instances is from the collections in [53]. To consider the skeleton of the interaction topology among the constituents in the networked systems, we remove self-loops (self-interaction of a constituent) and merge multi-edges (multiple interactions with the same direction between two constituents) in the network instances of the dataset.

TABLE I. A list of 24 real-world directed network instances. For each network, we show its type and name, a brief description, and its size of vertices (N) and arcs (M).

Type and Name	Description	N	M
Regulatory networks			
<i>E. coli</i> [54]	Transcriptional regulatory network of <i>E. coli</i> .	418	519
<i>S. cerevisiae</i> [55]	Transcriptional regulatory network of <i>S. cerevisiae</i> .	688	1,079
PPI networks			
PPI [56]	Protein-protein interaction network of human.	6,339	34,814
Metabolic networks			
<i>C. elegans</i> [57]	Metabolic network of <i>C. elegans</i> .	1,469	3,447
<i>S. cerevisiae</i> [57]	Metabolic network of <i>S. cerevisiae</i> .	1,511	3,833
<i>E. coli</i> [57]	Metabolic network of <i>E. coli</i> .	2,275	5,763
Neuronal networks			
<i>C. elegans</i> [58]	Neural network of <i>C. elegans</i> .	297	2,345
Food webs			
St Marks [59]	Food web in St. Marks River Estuary.	54	353
Everglades [60]	Food web in Everglades Graminoid Marshes.	69	911
Florida Bay [61]	Food web in Florida Bay.	128	2,106
Electronic circuits			
s208 [55]	Electronic sequential logic circuits.	122	189
s420 [55]	Same as above.	252	399
s838 [55]	Same as above.	512	819
Ownership networks			
USCorp [62]	Ownership network of US corporations.	7,253	6,724
Citation networks			
cit-HepTh [63]	Citation network in HEP-TH category of ArXiv.	27,769	352,768
cit-HepPh [63]	Citation network in HEP-PH category of ArXiv.	34,546	421,534
Internet p2p networks			
p2p-Gnutella04 [64, 65]	Gnutella peer-to-peer network from August 4, 2002.	10,876	39,994
p2p-Gnutella31 [64, 65]	Gnutella peer-to-peer network from August 31, 2002.	62,586	147,892
Web graphs			
Notre Dame [66]	Web graph of Notre Dame.	325,729	1,469,679
Stanford [67]	Web graph of Stanford.edu.	281,903	2,312,497
Google [67]	Web graph from Google.	875,713	5,105,039
Social networks			
WikiVote [68, 69]	Who-vote-whom network of Wikipedia users.	7,115	103,689
Epinions [70]	Who-trust-whom network of Epinions.com users.	75,879	508,837
Email-EuAll [64]	Email network from a EU research institution.	265,009	418,956

- [1] B. Bollobás, *Modern Graph Theory* (Springer, New York, 2002).
- [2] R. Albert and A.-L. Barabási, Statistical mechanics of complex networks, *Rev. Mod. Phys.* **74**, 47 (2002).
- [3] M. E. J. Newman, The structure and function of complex networks, *SIAM Review* **45**, 167 (2003).
- [4] S. Boccaletti, V. Latora, Y. Moreno, M. Chavez, and D.-U. Hwang, Complex networks: Structure and dynamics, *Phys. Rep.* **424**, 175 (2006).
- [5] S. N. Dorogovtsev, A. V. Goltsev, and J. F. F. Mendes, Critical phenomena in complex networks, *Rev. Mod. Phys.* **80**, 1275 (2008).
- [6] M. E. J. Newman, *Networks*, 2nd Edition (Oxford University Press, New York, 2018).
- [7] R. E. Kalman, Mathematical description of linear dynamical systems, *J. Soc. Indus. Appl. Math. A* **1**, 152 (1963).
- [8] C.-T. Lin, Structural controllability, *IEEE Trans. Automat. Contr.* **19**, 201 (1974).
- [9] Y.-Y. Liu, J.-J. Slotine, and A.-L. Barabási, Controllability of complex networks, *Nature* **473**, 167 (2011).
- [10] Y.-Y. Liu, J.-J. Slotine, and A.-L. Barabási, Control centrality and hierarchical structure in complex networks, *PLoS ONE* **7**, e44459 (2012).
- [11] M. Pósfai, Y.-Y. Liu, J.-J. Slotine, and A.-L. Barabási, Effect of correlations on network controllability, *Sci. Rep.* **3**, 1067 (2013).
- [12] T. Jia, Y.-Y. Liu, E. Csósa, M. Pósfai, J.-J. Slotine, and A.-L. Barabási, Emergence of bimodality in controlling complex networks, *Nat. Commun.* **4**, 2002 (2013).
- [13] S. P. Cornelius, W. L. Kath, and A. E. Motter, Realistic control of network dynamics, *Nat. Commun.* **4**, 1942 (2013).
- [14] T. Jia and M. Pósfai, Connecting core percolation and controllability of complex networks, *Sci. Rep.* **4**, 5379 (2014).
- [15] G. Menichetti, L. Dall'Asta, and G. Bianconi, Network Controllability is Determined by the Density of Low In-Degree and Out-Degree Nodes, *Phys. Rev. Lett.* **113**, 078701 (2014).
- [16] T. Nepusz and T. Vicsek, Controlling edge dynamics in complex networks, *Nat. Phys.* **8**, 568 (2012).
- [17] G. Yan, J. Ren, Y.-C. Lai, C.-H. Lai, and B. Li, Controlling Complex Networks: How Much Energy is Needed? *Phys. Rev. Lett.* **108**, 218703 (2012).
- [18] G. Yan, G. Tsekenis, B. Barzel, J.-J. Slotine, Y.-Y. Liu, and A.-L. Barabási, Spectrum of controlling and observing complex networks, *Nat. Phys.* **11**, 779 (2015).
- [19] Z. Yuan, C. Zhao, Z. Di, W.-X. Wang, and Y.-C. Lai, Exact controllability of complex networks, *Nat. Commun.* **4**, 2447 (2013).
- [20] J. Gao, Y.-Y. Liu, R. M. D'Souza, and A.-L. Barabási, Target control of complex networks, *Nat. Commun.* **5**, 5415 (2014).
- [21] J. Sun and A. E. Motter, Controllability Transition and Nonlocality in Network Control, *Phys. Rev. Lett.* **110**, 208701 (2013).
- [22] J. Ruths and D. Ruths, Control profiles of complex networks, *Science* **343**, 1373 (2014).
- [23] A. Li, S. P. Cornelius, Y.-Y. Liu, L. Wang, and A.-L. Barabási, The fundamental advantages of temporal networks, *Science* **358**, 1042 (2017).
- [24] A. Vinayagam, et al, Controllability analysis of the directed human protein interaction network identifies disease genes and drug targets, *Proc. Natl. Acad. Sci. USA* **113**, 4976 (2016).
- [25] G. Yan, P. E. Vértes, E. K. Towilson, Y. L. Chew, D. S. Walker, W. R. Schafer, and A.-L. Barabási, Network control principles predict neuron function in the *Caenorhabditis elegans* connectome, *Nature* **550**, 519 (2017).
- [26] Y.-Y. Liu and A.-L. Barabási, Control principles of complex systems, *Rev. Mod. Phys.* **88**, 035006 (2016).
- [27] L. Lovász and M. D. Plummer, *Matching Theory* (North-Holland, Amsterdam, 1986).
- [28] M. Mézard and A. Montanari, *Information, Physics, and Computation* (Oxford University Press, New York, 2009).
- [29] H.-J. Zhou and Z.-C. Ou-Yang, Maximum matching on random graphs, arXiv:cond-mat/0309348v1 [cond-mat.dis-nn] (2003).
- [30] L. Zdeborová and M. Mézard, The number of matchings in random graphs, *J. Stat. Mech.* (2006) P05003.
- [31] E. Kreačić and G. Bianconi, Statistical mechanics of bipartite z -matchings, arXiv:1810.10589 [cond-mat.dis-nn] (2018).
- [32] J. E. Hopcroft and R. M. Karp, An $n^{5/2}$ algorithm for maximum matchings in bipartite graphs, *SIAM J. Comput.* **2**, 225 (1973).
- [33] R. M. Karp and M. Sipser, Maximum matchings in sparse random graphs, in *Proceedings of the 22nd IEEE Annual Symposium on Foundations of Computer Science*, (Nashville, USA, October 1981), (IEEE, Piscataway, NJ, 1981), pp. 364-375.
- [34] J. Aronson, A. Frieze, and B. G. Pittel, Maximum matchings in sparse random graphs: Karp-Sipser revisited, *Random Struct. Alg.* **12**, 111 (1998).
- [35] D. Stauffer and A. Aharony, *Introduction to Percolation Theory*, Revised Second Edition (Taylor & Francis, London, 1994).
- [36] M. Bauer and O. Golinelli, Core percolation in random graphs: A critical phenomena analysis, *Eur. Phys. J. B* **24**, 339 (2001).
- [37] Y.-Y. Liu, E. Csóka, H.-J. Zhou, and M. Pósfai, Core Percolation on Complex Networks, *Phys. Rev. Lett.* **109**, 205703 (2012).
- [38] J.-H. Zhao and H.-J. Zhou, Two faces of greedy leaf removal procedure on graphs, arXiv:1809.05843 [physics.soc-ph] (2018).
- [39] M. Weigt and A. K. Hartmann, Number of Guards Needed by a Museum: A Phase Transition in Vertex Covering of Random Graphs, *Phys. Rev. Lett.* **84**, 6118 (2000).
- [40] M. Mézard, F. Ricci-Tersenghi, and R. Zecchina, Two solutions to diluted p -spin models and XORSAT problems, *J. Stat. Phys.* **111**, 505 (2003).
- [41] S. Cocco, O. Dubois, J. Mandler, and R. Monasson, Rigorous Decimation-Based Construction of Ground Pure States for Spin-Glass Models on Random Lattices, *Phys. Rev. Lett.* **90**, 047205 (2003).
- [42] L. Correale, M. Leone, A. Pagnani, M. Weigt, and R. Zecchina, Core Percolation and Onset of Complexity in Boolean Networks, *Phys. Rev. Lett.* **96**, 018101 (2006).

- [43] C. Lucibello and F. Ricci-Tersenghi, The statistical mechanics of random set packing and a generalization of the Karp-Sipser algorithm, *Intl. J. Stat. Mech.* 136829 (2014).
- [44] J.-H. Zhao, Y. Habibulla, and H.-J. Zhou, Statistical mechanics of the minimum dominating set problem, *J. Stat. Phys.* **159**, 1154 (2015).
- [45] Y. Habibulla, J.-H. Zhao, and H.-J. Zhou, The directed dominating set problem: Generalized leaf removal and belief propagation, edited by J. Wang and C. Yap, *FAW 2015: 9th International Frontiers of Algorithmics Workshop* (Guilin, China, 2015); Y. Habibulla, J.-H. Zhao, and H.-J. Zhou, *Lect. Notes Comput. Sci.* **9130**, 78 (2015).
- [46] P. Erdős and A. Rényi, On random graphs, I., *Publications Mathematicae* **6**, 290 (1959).
- [47] P. Erdős and A. Rényi, On the evolution of random graphs, *Publications of the Mathematical Institute of the Hungarian Academy of Sciences* **5**, 17 (1960).
- [48] A.-L. Barabási and R. Albert, Emergence of scaling in random networks, *Science* **286**, 509 (1999).
- [49] K.-I. Goh, B. Kahng, and D. Kim, Universal behavior of load distribution in scale-free networks, *Phys. Rev. Lett.* **87**, 278701 (2001).
- [50] M. Catanzaro and R. Pastor-Satorras, Analytic solution of a static scale-free network model, *Eur. Phys. J. B* **44**, 241 (2005).
- [51] J.-S. Lee, K.-I. Goh, B. Kahng, and D. Kim, Intrinsic degree-correlations in the static model of scale-free networks, *Eur. Phys. J. B* **49** 231 (2006).
- [52] <https://www.gnu.org/software/gsl/>.
- [53] J. Leskovec and A. Krevl, SNAP Datasets: Stanford Large Network Dataset Collection <http://snap.stanford.edu/data> (2014).
- [54] S. Mangan and U. Alon, Structure and function of the feed-forward loop network motif, *Proc. Natl. Acad. Sci. USA* **100**, 11980 (2003).
- [55] R. Milo, S. Shen-Orr, S. Itzkovitz, N. Kashtan, D. Chklovskii, and U. Alon, Network motifs: Simple building blocks of complex networks, *Science* **298**, 824 (2002).
- [56] A. Vinayagam, U. Stelzl, R. Foulle, S. Plassmann, M. Zenkner, J. Timm, H. E. Assmus, M. A. Andrade-Navarro, and E. E. Wanker, A directed protein interaction network for investigating intracellular signal transduction, *Science Signaling* **4**, rs8 (2011).
- [57] H. Jeong, B. Tombor, R. Albert, Z. N. Oltvai, and A.-L. Barabási, The large-scale organization of metabolic networks, *Nature* **407**, 651 (2000).
- [58] D. J. Watts and S. H. Strogatz, Collective dynamics of 'small-world' networks, *Nature* **393**, 440 (1998).
- [59] D. Baird, J. Luczkovich, and R. R. Christian, Assessment of spatial and temporal variability in ecosystem attributes of the St Marks National Wildlife Refuge, Apalachee Bay, Florida, *Estuarine, Coastal and Shelf Science* **47**, 329 (1998).
- [60] R. E. Ulanowicz, J. H. Heymans, and M. S. Egnotovich, Network analysis of trophic dynamics in South Florida Ecosystems (1445-CA09-95-0093 SA#2) FY 99: The Graminoid Ecosystem, annual report to the United States Geological Service, Biological Resources Division. Ref. No. [UMCES] CBL 00-0176, Technical Report No. TS-191-99, University of Maryland System, Chesapeake Biological Laboratory, Solomons, MD (2000).
- [61] R. E. Ulanowicz, C. Bondavalli, and M. S. Egnotovich, Network analysis of trophic dynamics in South Florida Ecosystems (1445-CA09-95-0093 SA#2) FY 97: The Florida Bay Ecosystem, annual report to the United States Geological Service, Biological Resources Division. Ref. No. [UMCES] CBL 98-123, University of Maryland System, Chesapeake Biological Laboratory, Solomons, MD (1998).
- [62] K. Norlen, G. Lucas, M. Gebbie, and J. Chuang, EVA: Extraction, visualization, and analysis of the telecommunications and media ownership network, in *Proceedings of International Telecommunications Society 14th Biennial Conference (ITS2002)*, Seoul Korea, August 2002 (ITS, Geneva, 2002), pp. 27-129.
- [63] J. Leskovec, J. Kleinberg, and C. Faloutsos, Graphs over time: Densification laws, shrinking diameters and possible explanations, in *Proceedings of the Eleventh ACM SIGKDD International Conference on Knowledge Discovery in Data Mining, Chicago, Illinois, USA, August 2005* (ACM, New York, 2005), pp. 177-187.
- [64] J. Leskovec, J. Kleinberg, and C. Faloutsos, Graph evolution: Densification and shrinking diameters *ACM Transactions on Knowledge Discovery from Data (TKDD)* Volume 1, Issue 1, Article No. 2, New York, NY, USA, March 2007 (ACM, New York, 2007).
- [65] M. Ripeanu, A. Iamnitchi, and I. Foster, Mapping the Gnutella network, *IEEE Internet Computing* **6**, 50 (2002).
- [66] R. Albert, H. Jeong, and A.-L. Barabási, Diameter of the World Wide Web, *Nature* **401**, 130 (1999).
- [67] J. Leskovec, K. J. Lang, A. Dasgupta, and M. W. Mahoney, Community structure in large networks: Natural cluster sizes and the absence of large well-defined clusters, *Internet Mathematics* **6**, 29 (2009).
- [68] J. Leskovec, D. Huttenlocher, and J. Kleinberg, Signed networks in social media, in *Proceedings of the SIGCHI Conference on Human Factors in Computing Systems, Atlanta, Georgia, USA, April 2010* (ACM, New York, 2010), pp. 1361-1370.
- [69] J. Leskovec, D. Huttenlocher, and J. Kleinberg, Predicting positive and negative links in online social networks in *Proceedings of the 19th International Conference on World Wide Web, Raleigh, North Carolina, USA, April 2010* (ACM, New York, 2010), pp. 641-650.
- [70] M. Richardson, R. Agrawal, and P. Domingos, Trust management for the semantic web, in *The Semantic Web - ISWC 2003*, edited by D. Fensel, K. Sycara, and S. Mylopoulos (Springer, New York, 2003); M. Richardson, R. Agrawal, and P. Domingos, *Lect. Notes Comput. Sci.* **2870**, 351 (2003).